Feedforward control for a temperature-robust toggle switch

Milo Knowles
mknowles@mit.edu

May 11, 2020

1 Problem Overview

In this project, the goal is to design a feedforward genetic circuit controller that can make the toggle switch robust to an increase in temperature. The circuit uses two mutually repressing proteins, which we denote as X_1 and X_2 in Figure 2, to implement a toggling behavior.

Under nominal conditions, this toggle switch circuit has two stable states in which one of the repressors has a high concentration, and the other has a low concentration. We model the temperature increase as an increase in the dissociation constant of the repressors. Effectively, this means that their repressive effect is weakened because they do not bind as strongly to their promoter targets. In Figure 1, we show that this can result in a loss of the bimodal toggle switch behavior. The goal of this project is to design a feedforward controller that can compensate for the effect of temperature and restore bimodality to the switch.

The toggle switch can be modelled by the following reduced-order ODEs, as derived in [1]:

$$\frac{dX_1}{dt} = \frac{\beta}{1 + (X_2/K)^2} - \gamma X_1 \tag{1}$$

$$\frac{dX_2}{dt} = \frac{\beta}{1 + (X_1/K)^2} - \gamma X_2 \tag{2}$$

where the constant K is a function of the dissociation constant K_d of the repressors.

2 Background and Related Works

2.1 Regulating Proteins through Controllable Protease Activity

In bacteria, a degradation tag can be added to the end of an amino acid sequence to trigger proteolysis. For example, Karzai et. al. [2] demonstrate that **ssrA** or "small stable RNA-A" can be attached to the C-terminus of proteins in *Escherichia coli* to trigger rapid degradation. Proteases such as **ClpX** or **ClpA** bind to the **ssrA**

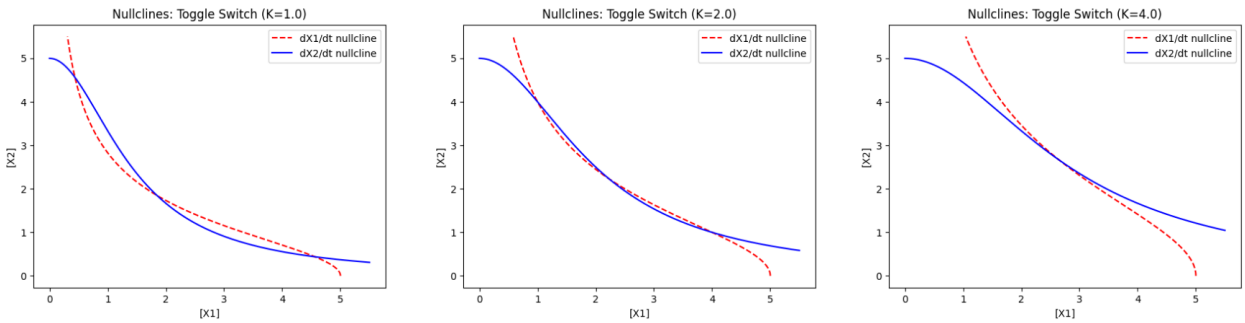

Figure 1: As the value of the dissociation constant increases (denoted by K in these plots), the shape of the nullclines changes. At a nominal dissociation constant, there are two stable equilibria, resulting in the desired bimodal behavior of the toggle switch. However, if the dissociation constant increases too much, as shown in the rightmost image, the nullclines lose the intersection points corresponding to these equilibria, and the system becomes monostable.

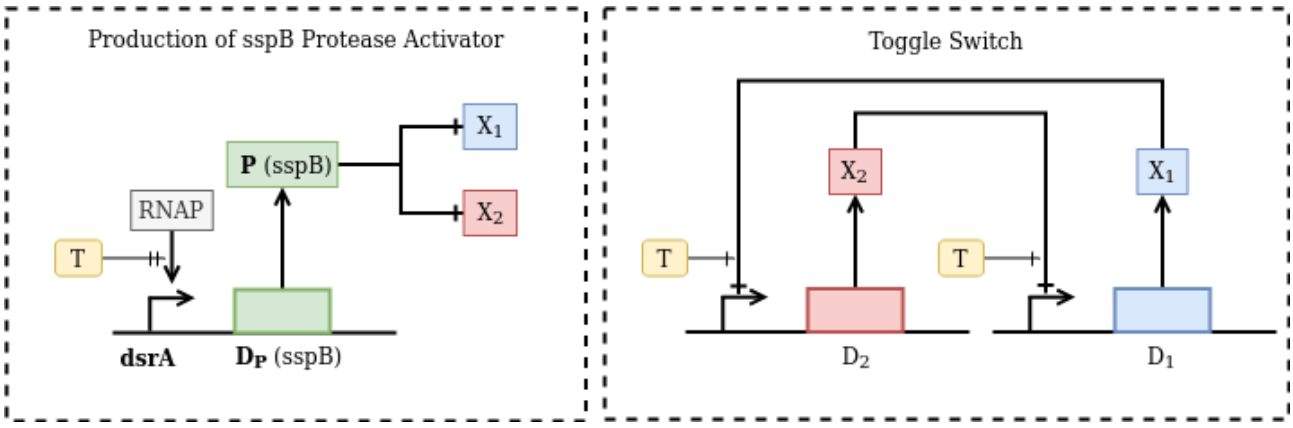

Figure 2: A simplified system diagram for the feedforward controller. **Left:** The **sspB** protease activator is expressed from a locus with the **dsrA** promoter sequence. Higher temperatures inhibit RNA polymerase from binding to the promoter region and initiating transcription. Once the **sspB** protein is translated, it binds to **ssrA** tags on X_1 and X_2, causing degradation via the **ClpX** protease. **Right:** A simplified diagram of the toggle switch model. X_1 and X_2 mutually repress each other by binding to the promoter. However, an increase in temperature increases the dissociation constant K_d, weakening the repressive effect of X_1 and X_2.

tag and denature the tagged protein.

This ability to trigger degradation through **ssrA** was extended by McGinness et. al. in [3] to allow more control over the degradation rate. These authors note that an adaptor protein **sspB** substantially increases degradation rates by binding to the **ssrA** tag and helping to recruit the **ClpX** protease. They modify the sequence of the **ssrA** tag to weaken ClpX binding while keeping the **sspB** binding affinity the same. This causes protein degradation via **ClpX** to work *only* in the presence of **sspB**, this making it controllable by changing the concentration of **sspB**.

2.2 Temperature Dependence of the dsrA Promoter

In [4], Repoila et. al. demonstrate that the **dsrA** promoter sequence has temperature sensing ability. This 36 base-pair promoter sequence binds RNA polymerase effectively at a temperature of 25C, but binds poorly at 42C. The authors hypothesis that, as temperature increases, the geometry of the promoter sequence is altered in a way that makes it more difficult for RNA polymerase to bind. Effectively, the dissociation constant of the **dsrA** promoter increases with higher temperature. In Section 3.1, we will refer to this dissociation constant as K_d^P.

3 Approach

Our insight is to use the temperature dependence of the **dsrA** promoter, in conjunction with the controllable **ssrA** + **sspB** protease system to compensate for an increase in temperature. First, we add the necessary **ssrA** tag sequence to the end of the DNA for the repressors X_1 and X_2, allowing us to target these proteins with the **ssrA** protease. In addition, we will place the **dsrA** promoter upstream of the **sspB** protease activator DNA. An increase in temperature will reduce the ability of RNA polymerase to bind to this promoter, such that the steady state concentration of **sspB** will be lower, and the degradation rate of the repressors will be reduced.

We can model this system as a feedforward controller that reduces the degradation rate of the repressors in response to an increase in temperature. In Section 4, we show that this can compensate for higher temperature by increasing the ratio β/γ, which restores bimodality to the toggle switch system. We provide a system diagram of the feedforward controller in Figure 2.

3.1 Nomenclature

3.1.1 Species

We consider the following species in our model:

- X_1 and X_2 are the mutually repressing proteins in the toggle switch

- X_1^d and X_2^d are the dimers of X_1 and X_2
- D_1 and D_2 are the DNA that express X_1 and X_2, respectively
- R is shorthand for RNA polymerase
- P is the protease activator **sspB**, and D_P is its DNA, which has the **dsrA** promoter
- D'_P is the transcriptionally active complex of R bound to D_P
- $C_{P,1}$ is the complex of P bound to X_1
- $C_{P,2}$ is the complex of P bound to X_2

3.1.2 Dissociation Constants

In addition, we define the following dissociation constants based on the reaction rate equations in Section 3.3:

- $K_d \triangleq \frac{k_4}{k_3}$ is the dissociation constant for the repressors
- $K_m \triangleq \frac{k_2}{k_1}$ is the dissociation constant for the dimers
- $K_d^P \triangleq \frac{k_8}{k_7}$ is the dissociation constant for the protease activator binding to the repressors
- $K_d^R \triangleq \frac{k_6}{k_5}$ is the dissociation constant for RNA polymerase binding to the **dsrA** promoter

3.2 Model Assumptions

- The toggle switch is symmetric, such that all reaction rate constants are the same for X_1 and X_2
- X_1 and X_2 can only repress each other in their dimer form (X_1^d and X_2^d)
- We model the expression of X_1, X_2, and P as a one-step reaction, ignoring mRNA dynamics
- We model the degradation of X_1 and X_2 as a two-step reaction (binding to the protease activator and then degrading). There is, in fact, a third step, where the protease activator recruits the **ClpX** protease. We will fold the dependence on the concentration of the **ClpX** protease into the the rate constant γ_P.

3.3 Modelling the Toggle Switch Reactions

In this section, we provide a simplified model of the reactions involved in the toggle switch and feedforward ontroller.

$X_1 \underset{k_2}{\overset{k_1}{\rightleftharpoons}} X_1^d$	Dimerization of X_1	(3)
$X_2 \underset{k_2}{\overset{k_1}{\rightleftharpoons}} X_2^d$	Dimerization of X_2	(4)
$X_1^d + D_2 \underset{k_4}{\overset{k_3}{\rightleftharpoons}} C_2$	X_1^d represses production of X_2	(5)
$X_2^d + D_1 \underset{k_4}{\overset{k_3}{\rightleftharpoons}} C_1$	X_2^d represses production of X_1	(6)
$D_1 \xrightarrow{\alpha_X} D_1 + X_1$	Translation of X_1, neglecting mRNA dynamics	(7)
$D_2 \xrightarrow{\alpha_X} D_2 + X_2$	Translation of X_2, neglecting mRNA dynamics	(8)
$X_1 \xrightarrow{\gamma} \phi$	Dilution of X_1	(9)
$X_2 \xrightarrow{\gamma} \phi$	Dilution of X_2	(10)
$R + D_P \underset{k_6}{\overset{k_5}{\rightleftharpoons}} D'_P$	RNA polymerase binds to the promoter of the protease activator P	(11)
$D'_P \xrightarrow{\alpha_P} R + D_P + P$	Translation of P from the active complex	(12)
$X_1 + P \underset{k_8}{\overset{k_7}{\rightleftharpoons}} C_{P,1}$	Protease activator P binds to X_1	(13)
$X_2 + P \underset{k_8}{\overset{k_7}{\rightleftharpoons}} C_{P,2}$	Protease activator P binds to X_2	(14)
$C_{P,1} \xrightarrow{\gamma_P} P + \phi$	Degradation of X_1 via the protease	(15)
$C_{P,2} \xrightarrow{\gamma_P} P + \phi$	Degradation of X_2 via the protease	(16)
$P \xrightarrow{\gamma} \phi$	Dilution of protease activator P	(17)
		(18)

3.4 Modelling the Effect of Temperature

- As stated in the project description, an increase in temperature results in an increase in the dissociation constant $K_d \triangleq \frac{k_4}{k_3}$ for the repressors X_1 and X_2 binding to their targets.
- Based on Section 2, an increase in temperature also increases the dissociation constant K_d^R for the RNA polymerase binding to the **dsrA** promoter. This results in a decrease in the expression of the protease activator **sspB**.

3.5 Reduced Order Models

3.5.1 Expression of the Protease Activator

In order for the protease activator P (**sspB**) to be expressed, RNA polymerase P must first bind to its DNA and form the transcriptionally active complex D'_P. We can write the following ODEs for the complex and protease activator:

$$\frac{dD'_P}{dt} = k_5 R(D_{P,tot} - D'_P) - k_6 D'_P \tag{19}$$

$$\frac{dP}{dt} = \alpha D'_P - \gamma P \tag{20}$$

Assuming quasi-steady-state, we get $D'_P = \frac{RD_{P,tot}}{R+K_d^R}$, where $K_d^R \triangleq \frac{k_6}{k_5}$ is the dissociation constant of RNA polymerase binding to the **dsrA** promoter.

Plugging the steady-state value for the complex D'_P into the expression for $\frac{dP}{dt}$, we can also solve for the equilibrium level of protease activator P:

$$P = \frac{RD_{P,tot}(\alpha_P/\gamma)}{R + K_d^R} \tag{21}$$

Based on Section 2, we assume that an increase in temperature will increase the dissociation constant K_d^R. In this form, it is easy to see that this will reduce the steady state amount of the protease activator P.

3.5.2 Degradation Due to the Protease Activator

As stated in Section 3.2, we assume a simplified two-step degradation of X_1 and X_2 that is activated by P. This is captured in the following ODEs:

$$\frac{dC_{P,1}}{dt} = k_7 P X_1 - k_8 C_{P,1} \tag{22}$$

$$\frac{dC_{P,2}}{dt} = k_7 P X_2 - k_8 C_{P,1} \tag{23}$$

$$\tag{24}$$

where we have ignored the effect of dilution, since the complex is formed at a much faster rate.

This gives the following expressions for the steady state concentration of the degradation complexes:

$$C_{P,1} = \frac{P X_1}{K_d^P} \tag{25}$$

$$C_{P,2} = \frac{P X_2}{K_d^P} \tag{26}$$

where $K_d^P \triangleq \frac{k_8}{k_7}$ is the dissociation constant for the protease activator P binding to X_1 and X_2.

We model the rate of protease-mediated degradation of X_1 and X_2 as being proportional to the concentration of the degradation complexes $C_{P,1}$ and $C_{P,2}$. This results in an additional term in the ODEs for the toggle switch model introduced in Section 1:

$$\frac{dX_1}{dt} = \frac{\beta}{1 + (X_2/K)^2} - X_1(\gamma + \gamma_P C_{P,1}) \tag{27}$$

$$= \frac{\beta}{1 + (X_2/K)^2} - X_1\left(\gamma + \gamma_P \frac{P}{K_d^P}\right) \tag{28}$$

$$= \frac{\beta}{1 + (X_2/K)^2} - X_1\left(\gamma + \frac{\gamma_P}{K_d^P}\frac{R D_{P,tot}(\alpha_P/\gamma)}{R + K_d^R}\right) \tag{29}$$

$$\frac{dX_2}{dt} = \frac{\beta}{1 + (X_1/K)^2} - X_2(\gamma + \gamma_P C_{P,2}) \tag{30}$$

$$= \frac{\beta}{1 + (X_1/K)^2} - X_2\left(\gamma + \gamma_P \frac{P}{K_d^P}\right) \tag{31}$$

$$= \frac{\beta}{1 + (X_1/K)^2} - X_2\left(\gamma + \frac{\gamma_P}{K_d^P}\frac{R D_{P,tot}(\alpha_P/\gamma)}{R + K_d^R}\right) \tag{32}$$

where to get Equations 29 and 32 we have plugged in the steady state expressions for $C_{P,1}$, $C_{P,2}$, and P.

We note that the constants β and K are an expression made up of several other constants. Based on the derivation in [1] (page 63), we include them here for completeness:

$$\beta = \frac{k_f [DNA_{tot}]([RNAP]/K_d^{RNAP})}{1 + ([RNAP]/K_d^{RNAP})} \tag{33}$$

$$K = (K_m K_d (1 + [RNAP]/K_d^{RNAP})^{1/2} \tag{34}$$

where K_d^{RNAP} is the dissociation constant for RNA polymerase binding to the DNA for X_1 and X_2, which we assume is *not* temperature-dependent. Here, $[DNA_{tot}]$ could correspond to $D_{1,tot}$ or $D_{2,tot}$, depending on whether this β is in the expression for $\frac{dX_1}{dt}$ or $\frac{dX_2}{dt}$.

Based on this expanded form of K, we see that K increases with the *square-root* of the temperature-dependent dissociation constant K_d.

3.6 Compensating for Increase in Temperature

Using the final form of the ODEs in Equations 29 and 32, we can see analytically how the feedforward controller compensates for an increase in temperature. Due the temperature sensing ability of the **dsrA** promoter

described in Section 2, the dissociation constant K_d^R increases at higher temperatures. As result, the steady state concentration of the protease activator P is reduced, causing the degradation of X_1 and X_2 to slow down. Numerically, this is captured by the K_d^R in the denominator of the degradation terms.

The "effective" gamma, which includes both dilution and degradation, is the expression $\gamma_{eff} \triangleq \gamma + \gamma_P \frac{P}{K_d^P}$. Thus, the increase in temperature will make this term smaller, and increase the ratio β/γ_{eff}. Visually, we demonstrate in Figure 3 that increasing this ratio compensates for the higher K and maintains the bimodality of the toggle switch.

4 Simulated Results

The code used to simulate these results is available at:
https://github.com/miloknowles/6.557-bio-feedback/tree/master/project

4.1 Nullcline Analysis

Using the ODEs in Equations 29 and 32, we perform nullcline analysis in Figure 3 to verify that the toggle switch and feedforward controller achieve the desired number of stable equilibria. We model increasing temperature by raising the values of K_d and K_d^R across a range of values. In all cases, K_d^R is proportional to K_d by a constant factor.

4.2 Stochastic Simulation

We also validate the proposed feedforward controller using the Stochastic Simulation Algorithm (SSA) [1]. In Figure 4, we examine the steady state joint probability distribution of X_1 and X_2 as we increase the dissociation constants K_d and K_d^R. As with the nullcline analysis, these dissociation constants increase proportionally. In our SSA implementation, we simulate one million reactions with the same dissociation constants used for the nullcline analysis. To generate the joint distribution histograms in Figure 4, we throw away the first 20 percent of reactions as burn-in samples, and then sample $20,000$ states uniformly across time.

5 Limitations

Although the results from nullcline and stochastic simulation demonstrate that the proposed system can compensate for modest increases in temperature, we found that the ability of a feedforward controller based on protease activity is fundamentally limited. In Section 3.6, we show that our controller reduces the steady state amount of the protease activator P, lowering the $\gamma_{eff} \triangleq \gamma + \gamma_P \frac{P}{K_d^P}$ term in order to compensate for a lower K_d. However, as the concentration of P approaches zero, γ_{eff} approaches γ, and is dominated by dilution. This means that our controller no longer has compensatory ability for very small P (i.e at very high temperatures). We see this empirically in Figure 3 and Figure 4 at the highest values of K_d.

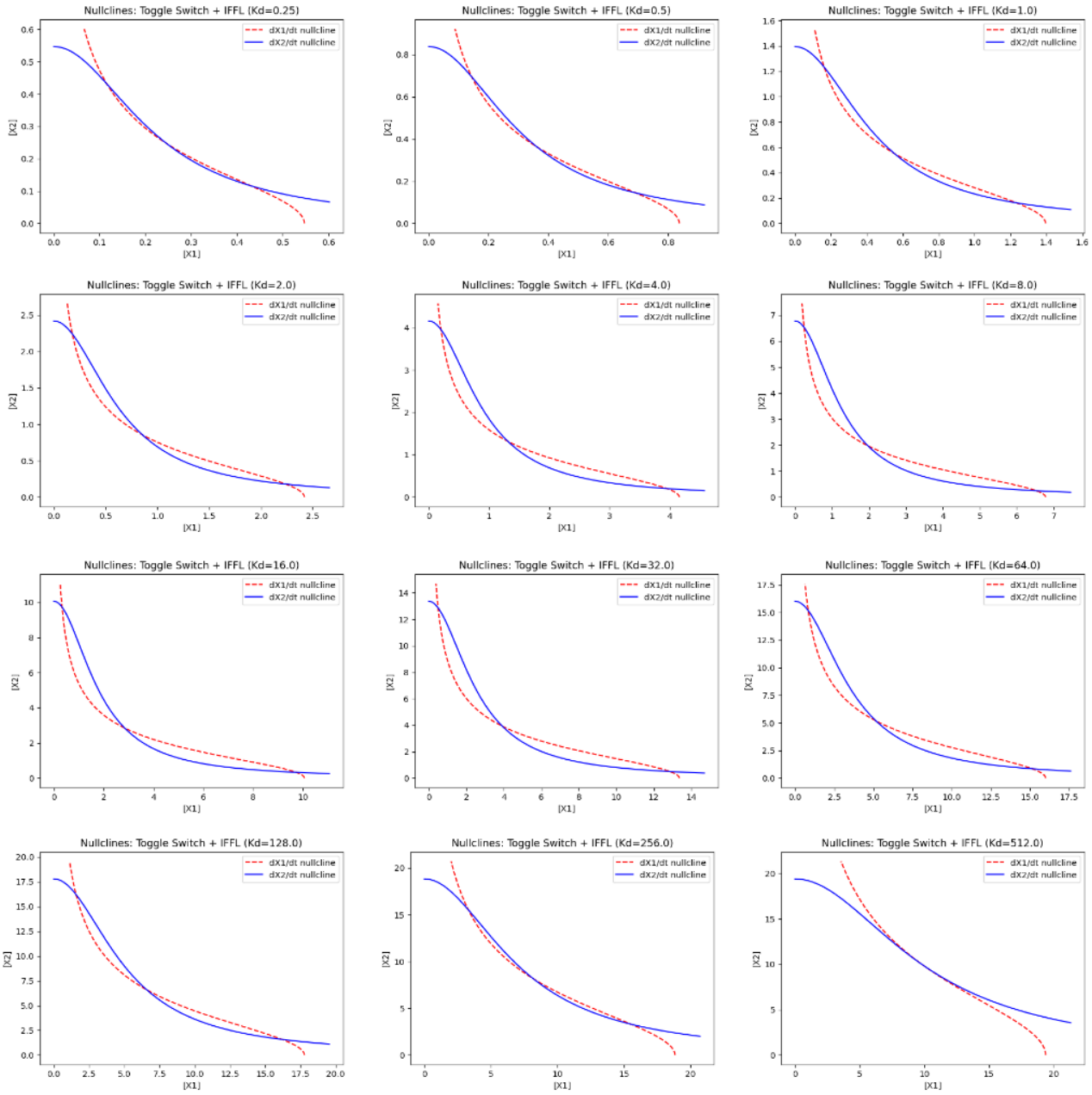

Figure 3: Nullcline analysis of the number of equilibria for different values of $K_d \in \{0.25, 0.5, 1, 2, 4, 8, 16, 32, 64, 128, 256, 512\}$. The proposed controller is robust to increases in K_d over two orders of magnitude, and the desired bimodal behavior is maintained up until $K = 256$. The ability of the controller to compensate for temperature is due to the fact that both K_d and K_d^R increase with temperature. As the dissociation constant K_d of the repressors increases, so does the dissociation constant K_d^R of RNA polymerase with the **dsrA** promoter region of the protease activator P. The amount of protease activator is reduced at higher temperatures, compensating for the higher K_d with a larger β/γ_{eff} ratio.

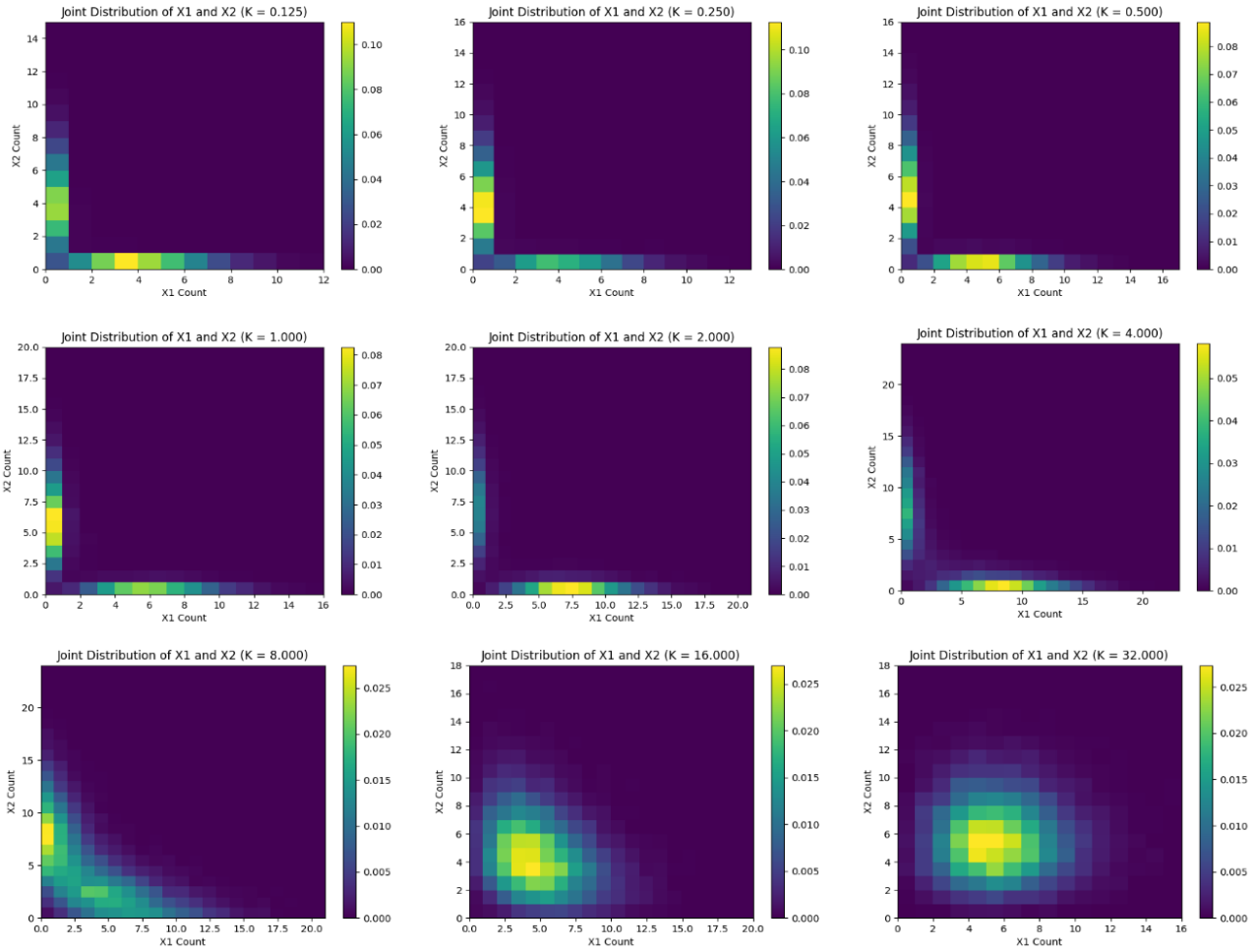

Figure 4: Joint probability distributions of X_1 and X_2 for increasing dissociation constants K_d and K_d^R. At low K_d values, the joint distribution demonstrates the desired bimodal toggle switch behavior. However, at $K_d = 8$, the peaks of the distribution become less distinct, and at $K = 16$ and $K = 32$, the distribution is unimodal. Interestingly, the nullcline analysis suggests that bimodal behavior should still be observed at these values of K_d, but we were unable to achieve this with stochastic simulation.

References

[1] Domitilla Del Vecchio and Richard Murray. Biomolecular Feedback Systems. 2015.

[2] A Wali Karzai, Eric D Roche, and Robert T Sauer. The SsrA–SmpB system for protein tagging, directed degradation and ribosome rescue. *Nature Structural Biology*, 7(6):449–455, jun 2000.

[3] Kathleen E McGinness, Tania A Baker, and Robert T Sauer. Engineering Controllable Protein Degradation. *Molecular Cell*, 22(5):701–707, jun 2006.

[4] F Repoila and S Gottesman. Temperature Sensing by the dsrA Promoter. *Journal of Bacteriology*, 185(22):6609–6614, 2003.